

Moving mass problem: Complete solution with the effect of initial conditions

Zuzana Dimitrovová^{1,2,*}

¹Departamento de Engenharia Civil, Faculdade de Ciências e Tecnologia, Universidade Nova de Lisboa, Portugal

²IDMEC, Instituto Superior Técnico, Universidade de Lisboa, Lisboa, Portugal

Abstract. In this contribution, recently published new semi-analytical solution for the moving mass problem [1] is extended to account for the transient terms that adapt the initial part of the complete solution in a way to match the initial conditions. It is assumed that a mass and a vertical force with harmonic component move by constant velocity along a horizontal infinite beam posted on a two-parameter visco-elastic foundation. The new semi-analytical solution is presented as a sum of truly steady-state terms, harmonic terms induced by the moving mass and transient terms adapting the initial conditions. Closed-form formula is given for the first two types of vibrations. It is concluded that transient terms have in most cases almost negligible effect on the full solution and that the initial conditions can significantly affect the amplitudes of the induced harmonic vibrations, but the induced frequencies are kept without any changes.

1 Introduction

Vibration analyses of beam structures under moving loads undoubtedly contributed to the design of modern railway lines. Deep understanding of dynamic phenomena related to train-track-soil interactions, and therefore, questions regarding the moving load and moving mass problems still attract the scientific community. New modelling approaches and solution methods are always welcomed to underline the necessary understanding. In this context, analytical and semi-analytical solutions have the unquestionable advantages of closed form solutions and quickly obtainable high-precision results solely in places of interest without the necessity to test numerical parameters ensuring the result convergence.

When the train passage is modelled by moving forces, then usually the critical velocity is the important feature to analyse. When inertia of the moving load is included, then additional feature as instability comes into account. Several authors have dedicated significant part of their research to instability of moving objects. Nevertheless, usually the main concern was on the identification of the instability interval, [2].

Considering the fact that someone may want to calibrate a numerical model, or control the unstable region, then it is pertinent not only to identify the instability velocity interval, but also determine the exact vibration pattern that will lead to instability. With this in mind the new semi-analytical solution was derived in closed form. The exact evolution of vibrations allows determining not only the onset of instability, but also its severity.

In Section 2 the problem is defined and solved. In Section 3 some examples and their validation are shown. The paper is concluded in Section 4.

2 Problem statement and solution

2.1. Assumptions

A uniform motion of a mass traversing a horizontal infinite beam posted on a two-parameter visco-elastic foundation is assumed. The beam has uniform cross section, its material is homogeneous and isotropic and it obeys linear elastic Euler-Bernoulli theory. It is further assumed that the moving mass is always in contact with the beam and no friction is considered at the contact point. The aim of the analysis is to determine full deflection shapes of the beam as a function of space and time, describing entirely the vertical vibrations induced by the moving mass and force. The problem at hand is depicted in Figure 1.

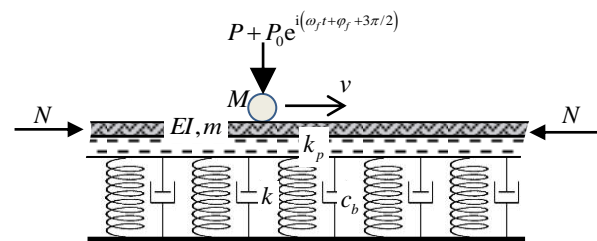


Fig. 1. Infinite beam on a visco-elastic two-parameter foundation subjected to a moving load and a normal force.

* Corresponding author: zdim@fct.unl.pt

In Figure 1 the following symbols are used: EI , m , and N stand for the bending stiffness and mass per unit length of the beam, and a normal force acting on the beam normal axis. k , k_p and c_b are Winkler's and Pasternak's moduli of the foundation and the coefficient of viscous damping of the foundation. Further in Figure 1, M designates the moving mass, P is the constant part of the moving force and the effect of the surface irregularity is approximated by a harmonic component with sine evolution in time t , which has an amplitude P_0 , a frequency ω_f and a phase angle φ_f . The harmonic part of the moving force is given more conveniently in the complex domain, thus the phase angle $\varphi_f + 3\pi/2$ is used to ensure the correspondence with $\sin(\omega_f t + \varphi_f)$. Finally, v is the constant velocity of the mass/force system.

2.2 Solution

At first, the deflection of the loading point is derived. Next, the full deflection shapes can be obtained by joining two semi-infinite beams. The solution procedure for the determination of the loading point displacement follows these steps: moving coordinate r is introduced; dimensionless parameters are substituted; Laplace transform in time is applied; Fourier transform in space is applied; and then the analytical form of the displacement image can be obtained and inverse Fourier transform can be applied in an analytical way to determine the Laplace image of the loading point displacement.

To simplify the expressions, a leading polynomial form can be designated as

$$D(p, q) = p^4 - 4p^2(\eta_N - \eta_S + \alpha^2) - 4q^2 + 8\alpha pq + 8i\eta_b q - 8i\eta_b \alpha p + 4 \quad (1)$$

where p and q are transformed variables: iq was used in Laplace transform in dimensionless time τ , thus corresponds to frequency; p was used in Fourier transform in dimensionless spatial coordinate ξ , thus corresponds to the transformed moving space coordinate. Other parameters are specified as

$$\eta_b = \frac{c_b}{2\sqrt{mk}}, \quad \eta_N = \frac{N}{2\sqrt{kEI}}, \quad \eta_S = \frac{k_p}{2\sqrt{kEI}}, \quad \xi = \chi r \quad (2)$$

$$\tau = \chi v_{cr} t, \quad \chi = \sqrt[4]{\frac{k}{4EI}}, \quad \alpha = \frac{v}{v_{cr}}, \quad v_{cr} = \sqrt[4]{\frac{4kEI}{m^2}} \quad (3)$$

where v_{cr} is the critical velocity of a constant force moving uniformly on the beam on Winkler's foundation k . Then the Laplace image of the loading point displacement is given by

$$\tilde{W}(0, iq) = -\frac{4i\left((q - \hat{\omega}_f)\eta_P + \eta_{P_0} q e^{i(\varphi_f + 3\pi/2)}\right)K(q)}{q(q - \hat{\omega}_f)(\pi - 2\eta_M q^2 K(q))} \quad (4)$$

where

$$\eta_M = \frac{M\chi}{m}, \quad \eta_P = \frac{P}{P} = 1, \quad \eta_{P_0} = \frac{P_0}{P}, \quad \hat{\omega}_f = \frac{\omega_f}{\chi v_{cr}} \quad (5)$$

and

$$K(q) = \int_{-\infty}^{\infty} \frac{dp}{D(p, q)}, \quad C(q) = \frac{4}{\pi} K(q) \quad (6)$$

where $C(q)$ is the frequency dependent flexibility of the foundation.

As the last step, the inverse Laplace transform is accomplished. This starts with the definition

$$f(t) = \frac{1}{2\pi i} \lim_{T \rightarrow \infty} \int_{a-iT}^{a+iT} e^{st} F(s) ds \quad (7)$$

where a is positive, real and greater than the real part of all singularities. In the expression above, the Laplace variable $s=iq$. Further, the variable s is switched to q and the final result is obtained by contour integration.

For correct application of the methods of the contour integration, it is necessary to analyse the behaviour of function $K(q)$. It is possible to conclude that the polynomial expression from Eq. (1) has always four complex roots and thus $K(q)$ can be obtained by the contour integration as well. The only exception is when $D(p, q)$ has real and multiple roots, which can only happen when $D(p, q)$ has real coefficients, which only occurs when $\text{Im}(q)=i\eta_b$. By further analysis it can be concluded that if certain two values of q have the same real parts and the imaginary parts are at the same distance from $i\eta_b$, then the corresponding $K(q)$ values are complex conjugates of each other. This also means that there is a discontinuity, or in other words, multiple value of $K(q)$ in complex q -plane along the horizontal line which crosses the imaginary axis at $i\eta_b$. In fact, by analysing the nature of the roots of $D(p, q)$ with real coefficients, it can be concluded, that there is a certain frequency, which can be called the "cutting frequency", q_C , for which $D(p, q)$ has multiple roots. The region with four complex roots is then limited by a certain velocity ratio a_C . For velocities lower than a_C there is an interval $(-q_C + i\eta_b, +q_C + i\eta_b)$ where the imaginary part of $K(q)$ is zero, which ensures continuity along the part of the line designated above as discontinuity line. Such region is, however, not identified for velocity ratio higher than a_C , and discontinuity in the imaginary part of $K(q)$ is satisfied along the full discontinuity line.

Due to the occurrence of multiple values as described above, the contour integration must be adapted in the way to avoid these regions. Thus

$$\tilde{w}_0(\tau) = \sum \text{res}(i\tilde{W}(0, q)e^{iq\tau}, q) + I_{bc} \quad (8)$$

where I_{bc} is the contribution obtained by the integration along the discontinuity regions, which can be named as branch cuts, however, their meaning is slightly different, because their position is not arbitrary. Other parts of the final result expressed in Eq. (8) are harmonic functions that are obtained by the sum of all residues. The type of residues additionally separates the solution to purely

steady state solution, that could be obtained by double Fourier transform, [3]. In this case it is composed by the residue at $q=0$, which represents the constant force contribution in form of

$$\widehat{w}_{0,1}(\tau) = \frac{4K(0)}{\pi} \eta_P \quad (9)$$

and by the residue at $q=\widehat{\omega}_f$, which represent the harmonic force contribution as

$$\widehat{w}_{0,2}(\tau) = \frac{4K(\widehat{\omega}_f) \eta_{P_0} e^{i(\varphi_f + 3\pi/2)}}{(\pi - 2K(\widehat{\omega}_f) \eta_M \widehat{\omega}_f^2)} e^{i\widehat{\omega}_f \tau} \quad (10)$$

Other harmonic parts must be added by the remaining residues. This is, however, not an easy task, because the poles must be determined as complex roots of complex equation, which reads

$$\pi = 2\eta_M q^2 K(q) \quad (11)$$

It is possible to conclude that in such a case the roots will always come in pairs, connected by

$$q_{M_2} = (-q_{M_1})^* \quad (12)$$

where * stand for complex conjugate value. Most commonly, there is only one pair of these roots, but there can be also two pairs or none. Having a root, q_M , the corresponding harmonic part is given by

$$\widehat{w}_{0,3}(\tau) = \frac{-2K(q_M) \eta_P}{q_M^3 K_{,q}(q_M) \eta_M + \pi} e^{iq_M \tau} \quad (13)$$

for the constant force and by

$$\widehat{w}_{0,4}(\tau) = \frac{-2q_M K(q_M) \eta_{P_0} e^{i(\varphi_f + 3\pi/2)}}{(q_M^3 \eta_M K_{,q}(q_M) + \pi)(q_M - \widehat{\omega}_f)} e^{iq_M \tau} \quad (14)$$

for the harmonic one.

2.3 Influence of the initial conditions

The solution presented in the previous section was directly derived for the homogeneous initial conditions. When these conditions are not homogeneous, then the application of the Laplace transform must be adapted accordingly. Changes must be introduced on both sides of the transformed governing equation. On the right-hand side, it must be simply added

$$4\eta_M (\widehat{w}_{, \tau}(0,0) + \overline{q} \widehat{w}(0,0)) \quad (15)$$

The other term, located on the left-hand side is not so easy to implement:

$$H(p,0) = -4\overline{W}_{, \tau}(p,0) - 4\overline{W}(p,0)(iq - 2i\alpha p + 2\eta_b) \quad (16)$$

Nevertheless, the leading effect can be attributed to the terms in Eq. (15) that directly express the initial conditions of the loading point and can significantly affect the amplitudes of the induced harmonics. For instance, the function for which residues are calculated in Eq. (8) for non-zero initial displacement and constant force changes to

$$\frac{2(2 - \eta_M q^2 \widehat{w}(0,0)) K(q) \eta_P}{q(\pi - 2\eta_M q^2 K(q))} e^{iq\tau} \quad (17)$$

which alters the contribution in Eq. (13) to

$$\widehat{w}_{0,3}(\tau) = \frac{-(2 - \eta_M q^2 \widehat{w}(0,0)) K(q_M) \eta_P}{q_M^3 K_{,q}(q_M) \eta_M + \pi} e^{iq_M \tau} \quad (18)$$

3 Examples

Examples presented in this section are related to railway applications. Only quite soft foundation is assumed, and the effect of Pasternak foundation, normal force and harmonic force is neglected. More details about these additional influences can be found in [1]. Moving force will be considered as a typical axle load, and for simplicity, the moving mass is assumed to have a value for which the moving force would represent the associated weight, according to approximate value of the gravity acceleration 10m/s². Nevertheless, dimensionless parameters are used and thus same results would be possible to obtain by different combinations of the input data. Values are listed in Table 1.

Table 1. Values used in numerical examples.

Property	Value
EI (10 ⁶ N m ²)	6.4
m (kg m ⁻¹)	60
k (10 ⁶ N m ⁻²)	1
P (10 ³ N)	100
M (kg)	10000

The associated characteristics and dimensionless values for this case are

$$v_{cr} = 290.4\text{m/s}, \chi = 0.445\text{m}^{-1}, \eta_M = 74.1 \quad (15)$$

Further, $w_{st}=0.022\text{m}$, which is the static displacement exerted by the constant part of the force on the beam on a Winkler foundation, that is used to obtain dimensionless displacements.

Firstly, the induced frequencies for the case of damping $\eta_b = 0.05$ are shown. These can be obtained by the iterative procedure described in [1]. Their evolution with velocity ratio is plotted in Figure 2. To each value shown there, another one exists in conformity with Eq. (12). It is seen that the values smoothly progress and the negative imaginary part, as the onset of instability is reached at $\alpha=1.07$. It is also seen that when discontinuity in $K(p,q)$ is reached, the frequency lines are cut. This happens when the imaginary part of the frequency reaches η_b , i.e. 0.05. This example was selected as an illustrative case, because there are certain velocity ratios for which none, one or two pairs of induced frequencies exist.

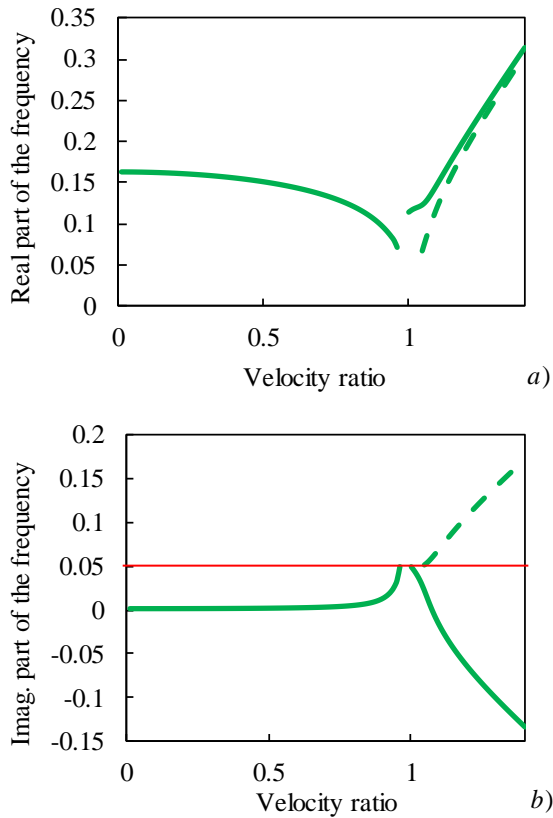


Fig. 2. Mass induced frequencies: a) the real part, b) the imaginary part.

Results for displacement evolution under the load are shown next. In all further figures validation on finite beams is presented as black dotted line. It is seen that the agreement between the results is excellent. In Figure 3 the case where only one pair of induced frequencies exists is shown. $\alpha = 0.344$ is selected (100m/s) and comparison is done for $\eta_b = 0$ and 0.1. It is seen that when there is no damping, there are large oscillations around the steady-state force displacement, with amplitude practically exactly equal to this steady state value. Such oscillations theoretically last for ever. When damping is included, these oscillations are gradually damped and after some time only the truly steady-state stage exists. In Figure 3 only the harmonic parts are plotted, namely the ones from Eq. (9) and (13), because the transient part is completely negligible. It was shown

in [4] that the transient part is important in this case only for low mass ratios, approximately equal to 10 or lower.

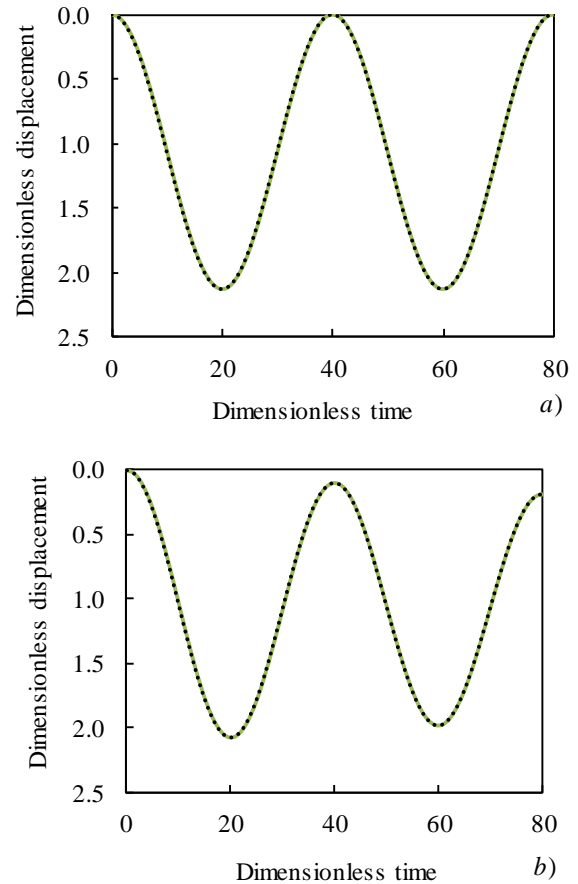


Fig. 3. Displacement under the load: a) $\eta_b = 0$, b) $\eta_b = 0.1$.

Next case is for $\eta_b = 0.05$. It is seen in Figure 2 that last one pair of frequencies occurs for $\alpha = 0.96$. Then for $\alpha = 0.97 - 0.99$ there are no induced frequencies, and one pair is gained again for $\alpha = 1$. This means that these cases must have significant contribution of the transient part, that needs to adjust the initial conditions. Results are shown in Figures 4, 5 and 6. In Figure 4 the case of $\alpha = 0.96$ is plotted.

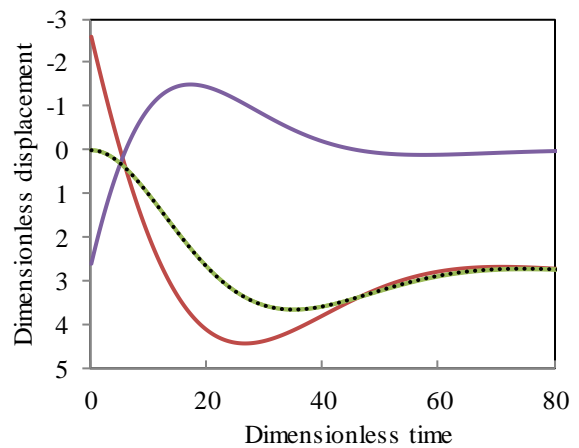


Fig. 4. Displacement under the load for $\alpha = 0.96$: harmonic part (red), transient part (violet), full solution (green).

It is seen in Figure 4 that the harmonic part starts at values very different from the initial conditions, therefore quite large values of the transient part must correct this fact. But the influence of the transient solution rapidly disappears.

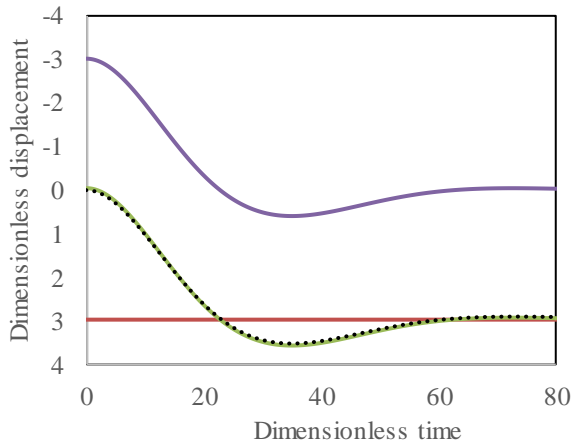


Fig. 5. Displacement under the load for $\alpha = 0.97$: harmonic part (red), transient part (violet), full solution (green).

In Figure 5 the case for $\alpha = 0.97$ is plotted. As there is no induced frequency, the harmonic part is constant, as it represents the steady-state solution only. Large influence of the transient solution corrects the initial conditions in the same way as before, and rapidly disappears.

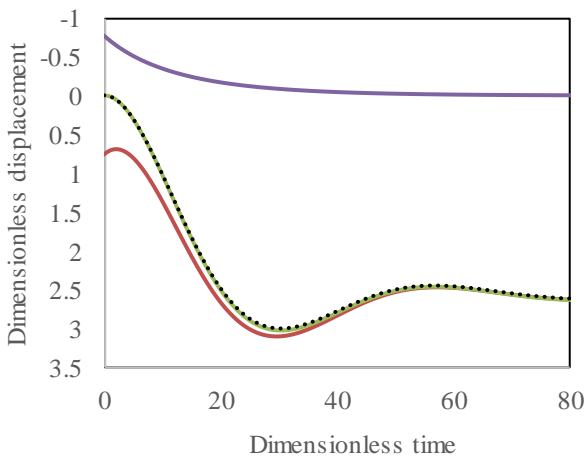


Fig. 6. Displacement under the load for $\alpha = 1$: harmonic part (red), transient part (violet), full solution (green).

When α reaches 1, there is again one pair of induced frequencies. This case is plotted in Figure 6. It is seen that as in all other cases, the transient part adjusts the initial conditions and then its effect over the solution is negligible.

Last example shown in this paper is the case when two pairs of induced frequencies exist. In such cases the second pair has always small influence on the solution, because it has large imaginary part, that is positive and thus quickly damp the vibration. Nevertheless, it is necessary to account for such solution, otherwise the

initial conditions would be violated. The case selected has $\eta_b = 0.2$ and $\alpha = 1.26$, which is the first velocity ratio where two pairs of induced frequencies occur for such level of damping. Results are shown in Figure 7.

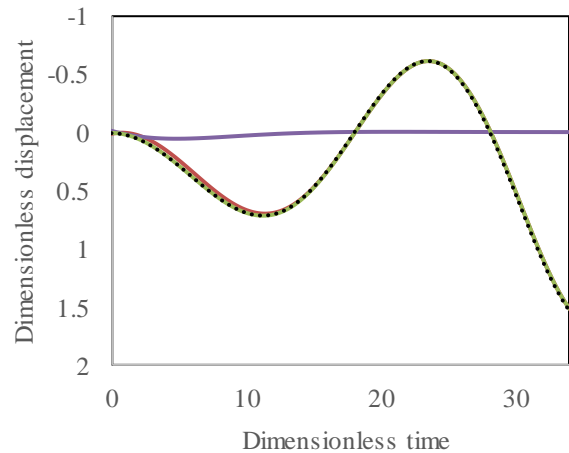


Fig. 7. Displacement under the load for $\alpha = 1.26$: harmonic part (red), transient part (violet), full solution (green).

In Figure 7 it is again seen that the transient part has negligible effect. The case selected belongs already to unstable vibrations, as can be verified by increasing amplitude of the vibrations. It can thus be concluded that the validity of the derived solution is not restricted to some specific velocity range.

4 Conclusion

In this paper closed form solution for moving mass problem was derived and validated. Several cases were discussed with respect to the number of induced pairs of frequencies and dominances of the distinct parts that compose the full solution.

This work was supported by FCT, through IDMEC, under LAETA, project UID/EMS/50022/2013.

References

1. Z. Dimitrovová, *Int. J. Mech. Sci.* **127**, 142–162 (2017).
2. A.V. Metrikine, H.A. Dieterman, *J. Sound Vib.*, **201**, 567–576 (1997).
3. S. Mackertich, *J. Acoust. Soc. Am.* **101**, 337–340 (1997).
4. Z. Dimitrovová, *Procedia Engineering* **199**, 2537–2542 (2017).